JOURNAL OF MATERIALS SCIENCE 26 (1991) 6809–6816

Diffusion-preventive Al_2O_3 layer growth at the interface of plasma-sprayed niobium and FeCrAlY in a tungsten fibre-reinforced high-temperature superalloy composite

S. OKUDE, M. ITOH, T. SUZUKI, M. NAKAHASHI
Metals and Ceramics Laboratory, Research and Development Centre, Toshiba Corporation, 1 Komukai Toshiba-Cho, Saiwaiku, Kawasaki 210, Japan

The growth mechanism of a diffusion-preventive layer formed at elevated temperatures (~1500 K) between the plasma-sprayed niobium layer and the plasma-sprayed FeCrAlY matrix in a tungsten fibre-reinforced high-temperature superalloy composite (Nb-coated W fibre/FeCrAlY composite) was studied. The diffusion-preventive layer was identified as α-Al_2O_3 by scanning electron microscopy/electron probe microanalysis, energy dispersive X-ray spectrometry analysis, and X-ray diffraction. Heat-treatment experiments were implemented systematically and it was found that the Al_2O_3 layer was also formed at the plasma-sprayed Nb/rolled FeCrAl interface. No Al_2O_3 layer, however, was formed either at the rolled Nb/plasma-sprayed FeCrAlY interface or at the rolled Nb/rolled FeCrAl interface. In these cases, an intermetallic compound layer was formed instead. A growth mechanism is proposed in which the Al_2O_3 is attributed to a chemical reaction between the residual oxygen in the plasma-sprayed niobium and aluminium in FeCrAlY or FeCrAl. The magnitude of the driving force was evaluated by a new model based on thermodyanamics. Numerical calculations have shown that the proposed growth mechanism is thermodynamically reasonable.

1. Introduction

Tungsten fibre/FeCrAlY composites are potentially useful as turbine blade materials because of their high strength at high temperatures [1, 2]. It combines the high creep strength property of the tungsten fibre and the high oxidation resistance property of the FeCrAlY superalloy. To retain a high creep strength at high temperatures, however, it is necessary to prevent chemical reactions between the tungsten fibre and the FeCrAlY matrix, because they cause a dramatic degradation of the creep property of the tungsten fibre [3].

We are now developing a niobium-coated tungsten fibre/FeCrAlY composite by using a low-pressure plasma spray-coating technique. In previously reported works [4–6] it was shown that (1) a thin (~1 μm) layer which prevents the diffusion of the FeCrAlY matrix elements (a diffusion-preventive layer) is formed between the niobium layer and the FeCrAlY matrix by heat treatment at an elevated temperature (~1500 K for several hours). The fibre degradation due to the fibre/matrix reaction is avoided by the diffusion-preventive layer; (2) no reaction occurs between the niobium layer and the tungsten fibre by heat treatment (~1500 K for several days) [2]; (3) on the other hand, no diffusion-preventive layer grows when a NiCoCrAlY matrix, which has an oxidation resistance property higher than that of FeCrAlY, is used instead of a FeCrAlY matrix. Neither chemical composition nor the growth mechanism of the diffusion-preventive layer, however, have been made clear. Their clarification has been required to establish a method for manufacturing a diffusion-preventive layer as an industrial production technology.

In the present work, the diffusion-preventive layer has been identified as α-Al_2O_3 by using scanning electron microscopy/energy dispersive X-ray spectrometry (SEM/EDX, for metallic elements), scanning electron microscopy/electron probe microanalysis (SEM/EPMA, for light elements) and X-ray diffraction (XRD) analyses. A direct XRD analysis of the thin and undulating Al_2O_3 layer has been realized by making it appear at the specimen surface by chemically etching away the FeCrAlY matrix. Heat-treatment experiments have shown that the diffusion-preventive layer grows at plasma-sprayed Nb/FeCrAlY interfaces but not at rolled Nb/FeCrAlY interfaces. An Al_2O_3 growth mechanism is proposed, in which a reaction between the residual oxygen in the plasma-sprayed niobium and aluminium in FeCrAlY is assumed. Numerical calculations have shown that the proposed growth mechanism is thermodynamically reasonable. The calculations also clarified the reason why no diffusion-preventive layer grows at the Nb/NiCoCrAlY interface.

0022-2461/91 \$03.00 + .12

TABLE I Conditions for low-pressure plasma spraying of niobium and FeCrAlY

	Plasma-spraying conditions	
	Nb	FeCrAlY
Atmospheric gas, Ar(Pa)	3.3×10^4	3.3×10^4
Plasma arc gas, Ar(Pa)	6.9×10^3	6.9×10^3
Supplemental gas, He(Pa)	6.9×10^3	6.9×10^3
Powder feeding gas, Ar(Pa)	6.9×10^3	6.9×10^3
Plasma spraying voltage (V)	37	36
Plasma spraying current, (A)	950	850
Distance between spray gun and specimen (mm)	325	325

2. Experimental procedure

The specimen used for identifying the diffusion-preventive layer was obtained by using a plasma-spraying method; a 0.1 mm thick niobium layer was first deposited on a 0.3 mm thick tungsten plate, and second a 0.1 mm thick FeCrAlY layer was deposited. An argon-fed powder plasma-spray gun was used to deposit niobium powder (CERAC: 99.8% pure, 10–44 μm diameter) and FeCrAlY powder (AMDRY: Fe–24Cr–8Al–0.5Y, 10–44 μm diameter) in a vacuum chamber filled with low-pressure (3.3×10^4 Pa) argon. The conditions for the low-pressure plasma-spraying of niobium and FeCrAlY are shown in Table I.

The composite thus obtained was enclosed in an evacuated fused-silica tube. A diffusion-preventive layer was formed by heat treatment of the enclosed composite at 1523 K for 9×10^4 s. A cross-section of the specimen was examined by SEM/EPMA and SEM/EDX analyses. The FeCrAlY layer was ultrasonically etched away in a concentrated HCl solution for 1.8×10^3 s and the diffusion-preventive layer was made to appear at the specimen surface before X-ray diffraction analysis.

Heat treatment (1473 K for 1.4×10^4 s) was systematically applied to the combinations of (plasma-sprayed or powder or rolled niobium)/(plasma-sprayed or powder FeCrAlY or rolled FeCrAl alloy). Then, the combinations for which a diffusion-preventive layer had formed were selected. The niobium powder and the FeCrAlY powder were the same as those used for the plasma-spraying material. The rolled FeCrAl alloy was (KANTAL) Type A-1, Fe–22Cr–5.8Al. The surfaces of the rolled niobium and the rolled FeCrAl alloy were finished by no. 1500 emery paper, and were cleaned ultrasonically in acetone. No further treatments were applied to the commercially obtained niobium powder or FeCrAlY powder.

An engineering work station (Toshiba AS4060) was used for the numerical calculations.

3. Results

3.1 Identification of the diffusion-preventive layer

Fig. 1 shows the SEM/EDX analysis results for a (plasma-sprayed niobium)/(plasma-sprayed FeCrAlY) interfacial region. A black zone, about 1 μm thick, observed in the scanning electron micrograph is the diffusion-preventive layer. No intermetallic reaction layer due to a Nb–FeCrAlY interaction is observed either in the niobium region or in the FeCrAlY region.

Fig. 2 shows the SEM/EPMA analysis result for a (plasma-sprayed niobium)/(plasma-sprayed FeCrAlY) interfacial region. The distributions of aluminium and oxygen completely coincide with the diffusion-preventive layer. This suggests that the diffusion-preventive layer is an Al_2O_3 layer.

Fig. 3 shows an XRD pattern for the diffusion-preventive layer, which was made to appear at the specimen surface. Strong peaks, corresponding to niobium, and small but clear peaks, corresponding to α-Al_2O_3, are observed. No other peaks are observed.

No niobium element was observed in the same exposed diffusion-preventive layer when qualitative analyses on metallic elements were carried out using EDX analysis. This means that the strong niobium peaks in Fig. 3 are attributed to the niobium layer underlying the diffusion-preventive layer, and not to the diffusion-preventive layer itself. These observations support the SEM/EPMA analysis of results shown in Fig. 2, i.e. that the diffusion-preventive layer is an Al_2O_3 layer.

3.2. Effect of the low-pressure plasma-spraying process on the diffusion preventive layer growth

Table II shows the combinations in which a diffusion-preventive layer is formed. It has been found that: (1) the layer is formed when the niobium layer is manufactured by plasma spraying, whether or not the FeCrAlY layer is manufactured by plasma spraying; (2) the layer is not formed when the niobium layer is powder or rolled niobium.

In the cases when no diffusion-preventive layer is formed, an intermetallic reaction layer about 10 μm thick is formed instead. As a typical example, a reaction layer formed between a rolled FeCrAl alloy and niobium powder is shown in Fig. 4. The chemical composition of the reaction layer, which was determined by quantitative analysis by EDX, is shown in Table III. It shows that the main elements in the intermetallic reaction layer are iron and niobium.

4. Discussion

4.1. Growth mechanism of a diffusion-preventive layer

It is well known that a metal layer deposited by plasma-spraying methods contains a considerable amount of residual oxygen (approximately atomic per cent). The present experimental results indicate that a diffusion-preventive layer (Al_2O_3 layer) grows only

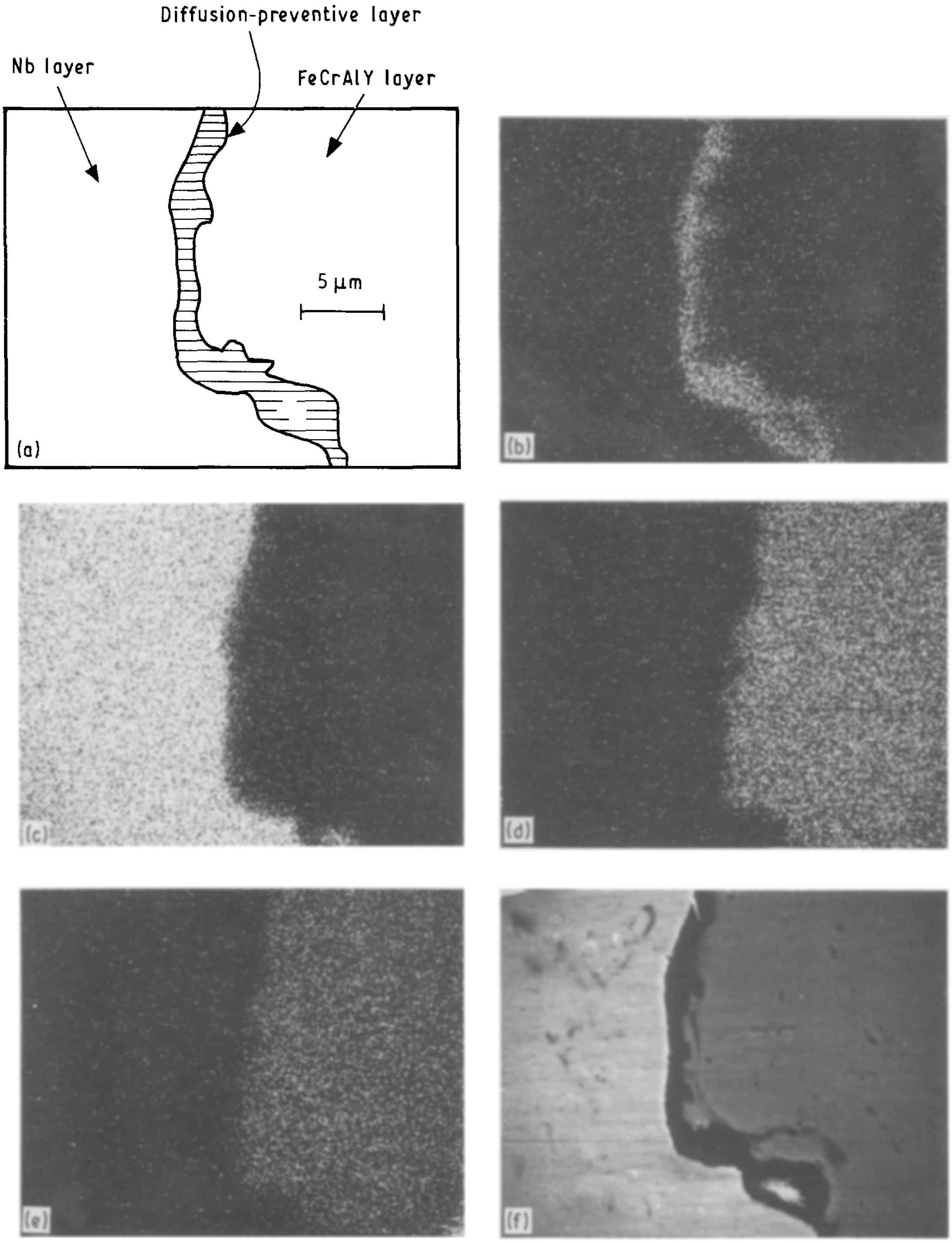

Figure 1 (a) SEM/EDX analysis of (plasma-sprayed Nb)/(plasma-sprayed FeCrAlY) interfacial region. (b–e) Distributions of metallic elements (Al, Nb, Fe, and Cr, respectively) are shown. A black zone about 1 μm thick observed in the micrograph (f) indicates a diffusion-preventive layer. No intermetallic reaction layer showing Nb–FeCrAl interaction is observed.

when plasma-sprayed niobium is used. We propose a growth mechanism in which Al_2O_3 layer growth is attributed to a chemical reaction between the residual oxygen in niobium and aluminium in FeCrAlY.

In typical heat-treatment experiments, an Al_2O_3 layer about 1 μm thick grows from a niobium layer about 100 μm thick. If the oxygen in Al_2O_3 is mainly supplied from the niobium layer, niobium must have contained at least 1–2 at % residual oxygen. The solid solubility limit of oxygen in niobium is 4.0 at % at 2188 K and 1.43 at % at 773 K [7], and would be still lower at room temperature. Some of the residual oxygen in plasma-sprayed niobium is expected to be in niobium oxide form (NbO) at room temperature if thermodynamic equilibrium is achieved.

The porosity of a plasma-sprayed layer is generally less than 1 vol %. Even if pure oxygen gas at atmospheric pressure is contained in it, the amount of oxygen is one-thousandth of that needed to form a 1 μm thick Al_2O_3 layer. Therefore, the oxygen from porosity does not play a significant role in Al_2O_3 growth.

For a quantitative discussion, we considered two criteria for the growth of a diffusion preventive layer:

(1) the growth of an Al_2O_3 layer is thermodynamically allowed (thermodynamic criterion);

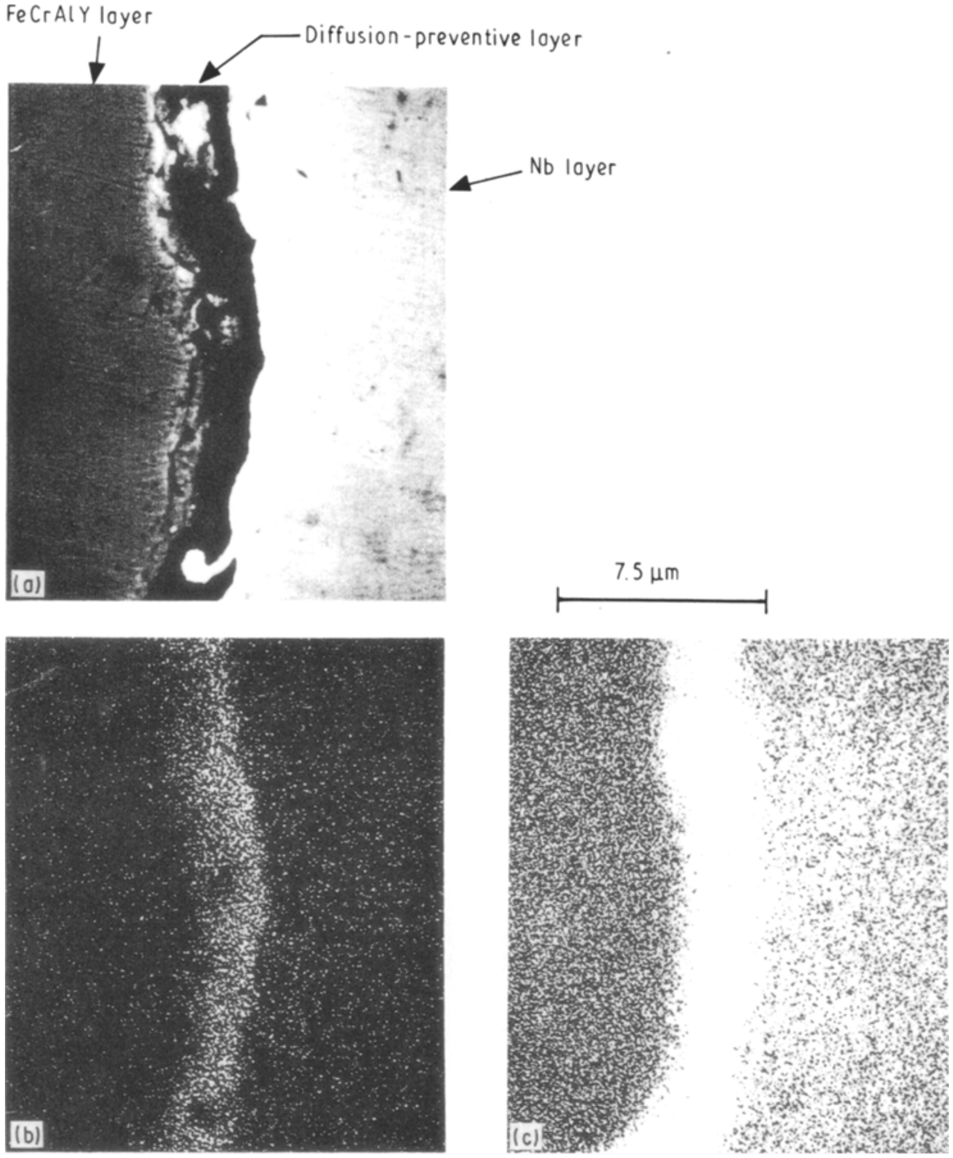

Figure 2 (a) SEM/EPMA analysis of (plasma-sprayed Nb)/(plasma-sprayed FeCrAlY) interfacial region. Distributions of (b) oxygen and (c) aluminium elements are shown. These distributions coincide with the diffusion-preventive layer. This suggests that the diffusion-preventive layer is an Al_2O_3 layer.

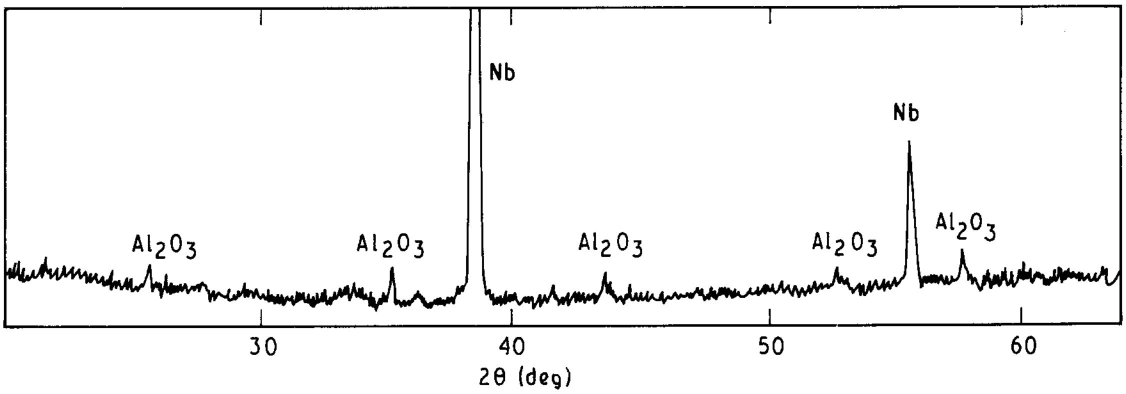

Figure 3 X-ray diffraction pattern of a diffusion-preventive layer made to appear at the specimen surface by chemical etching. Clear peaks due to α-Al_2O_3 of the diffusion-preventive layer are observed. The strong niobium peaks are due to the niobium layer, which underlies the diffusion-preventive layer.

(2) the reaction rate of the Al_2O_3 layer growth dominates over those of other competing chemical reactions, such as $2Fe + Nb \rightarrow Fe_2Nb$ (reaction rate criterion).

The thermodynamic criterion is too loose to be used as a strict condition regarding the Al_2O_3 layer growth. Its theoretical treatment, however, is simpler than that for the reaction rate criterion, and is suitable to be used to clarify the outline of the phenomenon. So, the thermodynamic criterion is discussed first.

TABLE II Combinations in which a diffusion-preventive layer is formed

	FeCrAlY		
	Powder	Plasma sprayed	Rolled
Powder	–	–	×
Plasma sprayed	–	○	○
Rolled	×	×	×

○, Layer formed.
×, Layer not formed.
–, Not measured.

TABLE III Chemical composition of intermetallic reaction layer formed between rolled FeCrAlY alloy and powder niobium

Element	(at %)
Fe	56
Cr	12
Al	3
Nb	29

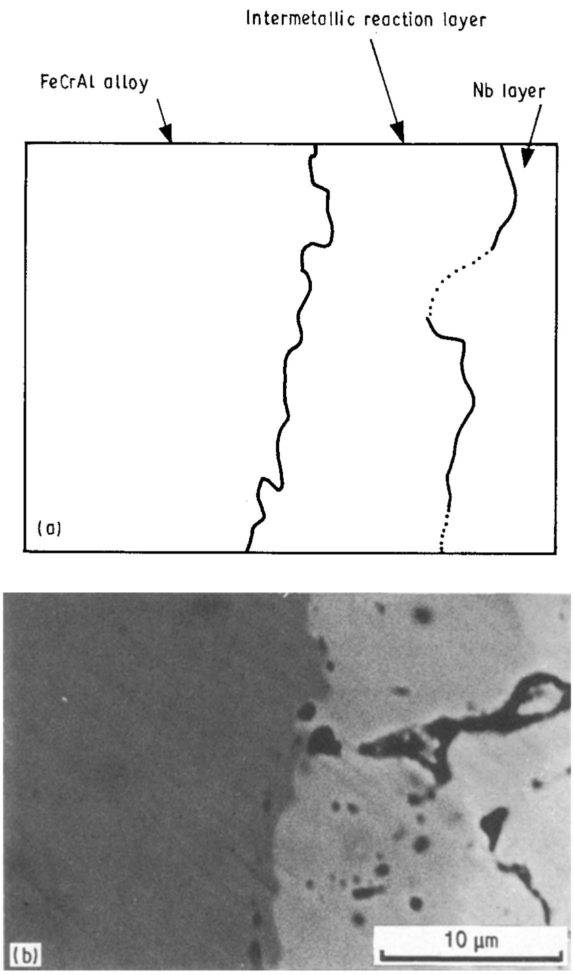

Figure 4 Intermetallic reaction layer formed between rolled FeCrAl alloy and niobium powder. No diffusion-preventive layer is observed.

4.2. Thermodynamic criterion for the growth of an Al_2O_3 layer

A thermodynamical model was used to obtain a criterion for the Al_2O_3 layer growth. In this model, an iron-base substitutional solid solution, FeCrAlY, was simplified to a binary alloy, Al/Fe (aluminium dissolved in iron), and a nickel-base substitutional solid solution, NiCoCrAlY, was simplified to a binary alloy, Al/Ni (aluminium dissolved in nickel).

First, a chemical reaction between Al/Fe and O/Nb (oxygen dissolved in niobium) is discussed. Usually, a chemical reaction of

$$2\text{Al/Fe} + 3\text{O/Nb} \rightarrow \text{Al}_2\text{O}_3 \qquad (1)$$

is employed to discuss a thermodynamic criterion. This reaction is judged as "thermodynamically allowed" if the change in the Gibbs energy has a negative value

$$\Delta G_{\text{Al/Fe–O/Nb}}(X_{\text{Al/Fe}}, X_{\text{O/Nb}}, T) < 0 \qquad (2)$$

where $X_{\text{Al/Fe}}$ is the density of aluminium in iron, $X_{\text{O/Nb}}$ is the density of oxygen in niobium, and T is the temperature.

It should be noted that Equation 1 indicates a chemical reaction, in which an Al–Fe solid solution containing 2 mol Al and an O–Nb solid solution containing 3 mol O reacts completely, and 1 mol Al_2O_3, pure iron, and pure niobium are formed. Equation 2 is a criterion for the possibility of the completion of the reaction, and is too strict as a criterion for the possibility of the initiation of the reaction.

So, instead of the reaction in Equation 1, a reaction at the initial stage of Al_2O_3 formation is employed to discuss a thermodynamic criterion; in this reaction, a minimal amount of Al_2O_3 is formed. With this, the density of aluminium in iron and the density of oxygen in niobium decrease by minimal amounts. That is,

$$\begin{aligned}&[X_{\text{Al}}\text{Al} + X_{\text{Fe}}\text{Fe}] + [X_{\text{O}}\text{O} + X_{\text{Nb}}\text{Nb}]\\ &\quad\rightarrow \delta X\,\text{Al}_2\text{O}_3 + [(X_{\text{Al}} - 2\delta X)\text{Al}\\ &\qquad + X_{\text{Fe}}\text{Fe}] + [(X_{\text{O}} - 3\delta X)\text{O} + X_{\text{Nb}}\text{Nb}]\end{aligned} \qquad (3)$$

where $[X_{\text{Al}}\cdot\text{Al} + X_{\text{Fe}}\cdot\text{Fe}]$ means a solid solution composed of X_{Al} mol Al and X_{Fe} mol Fe, and $[X_{\text{O}}\text{O} + X_{\text{Nb}}\text{Nb}]$ means a solid solution composed of X_{O} mol O and X_{Nb} mol Nb.

The change in the Gibbs free energy for Equation 3 is given by

$$\begin{aligned}&\Delta G_{[X_{\text{Al}}\text{Al} + X_{\text{Fe}}\text{Fe}][X_{\text{O}}\text{O} + X_{\text{Nb}}\text{Nb}]}(X_{\text{Al}}, X_{\text{Fe}}, X_{\text{O}}, X_{\text{Nb}}, \delta X, T)\\ &\quad = \delta X\,\Delta G_{\text{Al}_2\text{O}_3}(T)\\ &\qquad + \Delta G_{\text{Al–Fe}}(X_{\text{Al}} - 2\delta X, X_{\text{Fe}}, T)\\ &\qquad + \Delta G_{\text{O–Nb}}(X_{\text{O}} - 3\delta X, X_{\text{Nb}}, T)\\ &\qquad - \Delta G_{\text{Al–Fe}}(X_{\text{Al}}, X_{\text{Fe}}, T)\\ &\qquad - \Delta G_{\text{O–Nb}}(X_{\text{O}}, X_{\text{Nb}}, T)\end{aligned} \qquad (4)$$

where $\Delta G_{\text{Al}_2\text{O}_3}(T)$ is the Gibbs free energy for the formation of 1 mol Al_2O_3, $\Delta G_{\text{Al–Fe}}(X_{\text{Al}}, X_{\text{Fe}}, T)$ is the Gibbs free energy for the formation of $[X_{\text{Al}}\text{Al} + X_{\text{Fe}}\text{Fe}]$, and $\Delta G_{\text{O–Nb}}(X_{\text{O}}, X_{\text{Nb}}, T)$ is the Gibbs free energy for the formation of $[X_{\text{O}}\text{O} + X_{\text{Nb}}\text{Nb}]$.

The numerical values for $\Delta G_{\text{Al–Fe}}$, $\Delta G_{\text{O–Nb}}$, and $\Delta G_{\text{Al}_2\text{O}_3}$ are determined by using pertinent literature values [7–9]. To describe the Gibbs free energy for the formation of a component of a solid solution as a function of the component density, x, and temperature, T, an equation is used in the form of

$$\Delta G = \Delta G^0 + RT\ln(x) \qquad (5)$$

To describe the pertinent literature value by Equation 5, the x dependence of ΔG^0 is empirically introduced by interpolation. The temperature dependence of the Gibbs free energy is introduced by interpolation when there are literature values concerning such temperature dependence for the material. Otherwise, the temperature dependence is introduced by integrating the Gibbs–Helmholtz equation over temperature, ignoring the temperature dependence of enthalpy.

A differential value, $\Delta\mu$, is defined by

$$\Delta\mu = (\partial/\partial\,\delta X)\Delta G_{[X_{Al}Al + X_{Fe}Fe][X_O O + X_{Nb}Nb]} \times (X_{Al}, X_{Fe}, X_O, X_{Nb}, \delta X, T) \qquad (6)$$

The thermodynamic criterion for the initiation of Al_2O_3 growth is given by

$$\Delta\mu < 0 \qquad (7)$$

The temperature versus O/Nb density region is calculated numerically, in which the thermodynamic criterion in Equation 7 is broken (see Fig. 5). The black region in Fig. 5 indicates the growth-forbidden region for the Al/Fe–O/Nb system. The hatched area indicates the growth-forbidden region for the Al/Ni–O/Nb system. The whole contour of the hatched area is given in Fig. 6, in which the growth-forbidden region is given for a wider range of atomic per cent oxygen in niobium compared with that in Fig. 5. In this numerical calculation, we set $X_{Fe}/X_{Nb} = 1$, and $X_{Ni}/X_{Nb} = 1$, because the widths of the FeCrAlY layer, NiCoCrAlY layer, and the niobium layer were comparable with one another. The result of the numerical calculation, however, is insensitive to the values of X_{Fe}/X_{Nb} or X_{Ni}/X_{Nb} even when these values are changed by several factors. The value for "atomic per cent oxygen in niobium" on the boundary line in the "growth-forbidden region" changes only by less than 1% in absolute value.

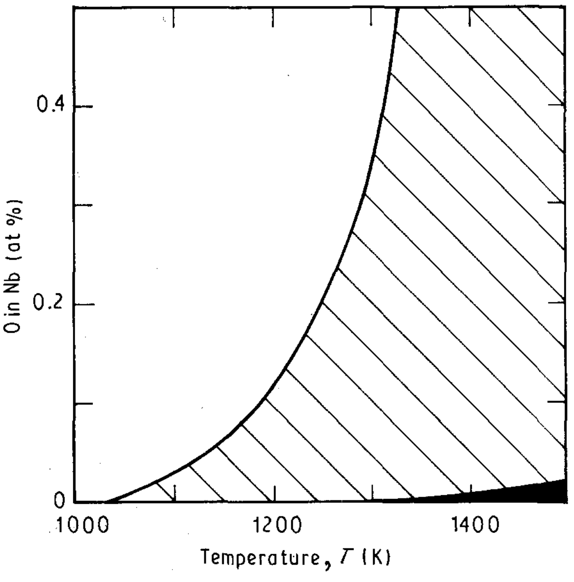

Figure 5 Regions where the growth of a diffusion-preventive layer is forbidden by the thermodynamic criterion in Equation 7. The growth-forbidden region for the Al/Ni–O/Nb system (hatched area) is much wider than that for the Al/Fe–O/Nb system (black region).

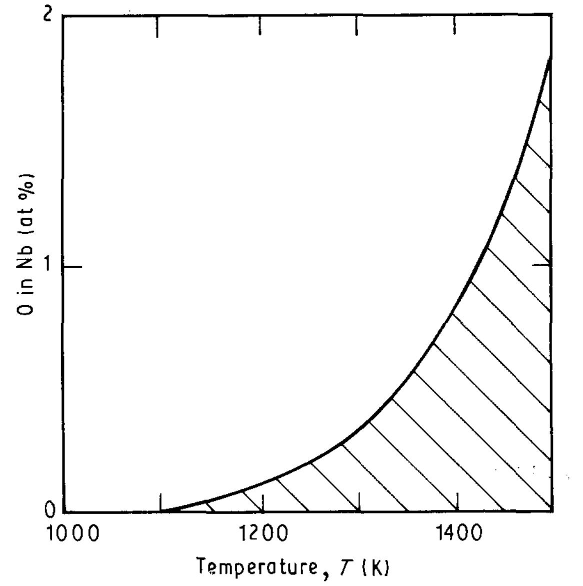

Figure 6 Regions where the growth of a diffusion-preventive layer is forbidden by the thermodynamic criterion in Equation 7. The range of atomic per cent oxygen in niobium shown in this figure is larger than that shown in Fig. 5. The entire contour of the growth-forbidden region for Al/Ni–O/Nb (hatched area) is shown. The growth-forbidden region for Al/Fe–O/Nb is too small to be shown in this figure.

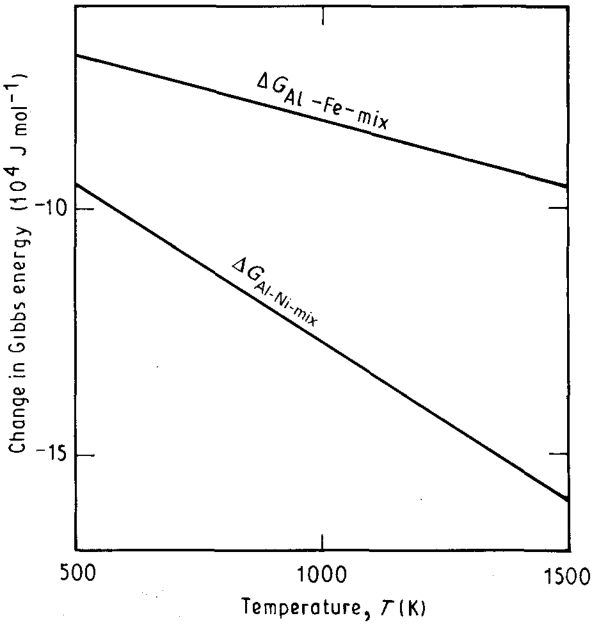

Figure 7 Change in Gibbs free energy by mixing 1 mol Al with iron or nickel. The density of aluminium in Al/Fe is set at 15 at %, and that of aluminium in Al/Ni is set at 24 at %. The plot for Al/Ni is beneath that for Al/Fe. This shows that Al/Ni is thermodynamically more stable than Al/Fe.

The density of aluminium in iron was set equal to that of aluminium in the plasma-spray powder, FeCrAlY (15 at %). The density of aluminium in nickel was set equal to that of a plasma-spray powder, NiCoCrAlY (24 at %).

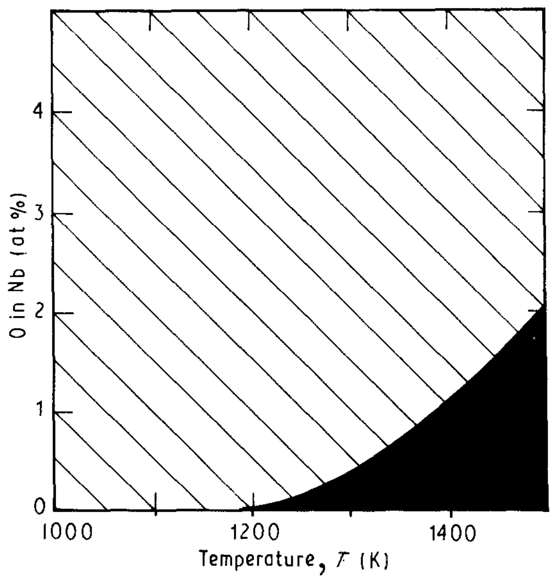

Figure 8 Regions where the growth of a diffusion-preventive layer is forbidden by the conventional thermodynamic criterion in Equation 2. Both the growth-forbidden region for the Al/Ni–O/Nb system (hatched area) and that for the Al/Fe–O/Nb system (black region) are wider than those given by the present thermodynamic criterion of Equation 7 (Fig. 5).

Figs 5 and 6 show that the growth-forbidden region for the Al/Fe–O/Nb system is much narrower than that for the Al/Ni–O/Nb system. This result is consistent with the experimental result wherein the Al_2O_3 layer grows in the Nb/FeCrAlY system, but does not grow in the Nb/NiCoCrAlY system.

The wide growth-forbidden region for the Al/Ni–O/Nb system is caused by the thermodynamic stability of the Al/Ni solid solution. It is difficult for aluminium dissolved in nickel to be separated from a stable Al/Ni solid solution and to form Al_2O_3.

The stability of the Al/Ni solid solution compared with that of the Al/Fe solid solution is shown in Fig. 7, in which the change in the Gibbs free energy by mixing 1 mol Al with iron or nickel as a function of temperature is plotted. In the numerical calculation to obtain Fig. 7, the density of aluminium in Al/Fe is set at 15 at %, and that of aluminium in Al/Ni is set at 24 at %. The plot for the Al/Ni solid solution lies beneath the plot for the Al/Fe solid solution. This shows that the Al/Ni solid solution is thermodynamically more stable than the Al/Fe solid solution.

Fig. 8 shows the growth-forbidden region calculated by the conventional criterion. The conventional growth-forbidden region in Fig. 8 is wider compared with the present criterion (Fig. 5). This is because the conventional criterion is the condition for the "completion" of a chemical reaction and is much more strict than the present criterion for the "initiation" of the reaction.

4.3. Reaction-rate criterion for the growth of the Al_2O_3 layer

The main interfacial reaction which competes with the Al_2O_3 growth at the Al/Fe–O/Nb interface is

$$2Fe + Nb \rightarrow Fe_2Nb \qquad (8)$$

We made a rough estimation as to which of the two reactions (Equation 3 or 8) proceeds faster and dominates the other. In this estimation, the change in the Gibbs free energy per atom of the reaction products is calculated; that is, $\Delta G_{2Fe\text{-}Nb}/(2 + 1)$ for Fe_2Nb, and $\Delta\mu/(2 + 3)$ for Al_2O_3.

The Al_2O_3 growth is judged to dominate over the Fe_2Nb growth if $|\Delta\mu/5| > |\Delta G_{2Fe\text{-}Nb}/3|$ is satisfied. In this judgment, the possibility of the existence of a "transient state", which is discussed in a detailed theory of rate processes, is neglected.

A numerical estimation was made in the temperature region ~1500 K, where the heat treatments were carried out. The result shows that Al_2O_3 growth dominates over Fe_2Nb growth when the density of the residual oxygen in niobium is more than 1–2 at %. In general, residual oxygen of the order of a few per cent is often taken into metals during a plasma-spraying process for metals. Therefore, it is reasonably expected that the plasma-sprayed niobium layer would contain enough oxygen density for the domination of Al_2O_3 growth. This result supports the growth mechanism proposed in Section 4.1, i.e. that the Al_2O_3 layer grows by a reaction between the residual oxygen in niobium and aluminium in FeCrAlY.

For comparison with the present calculation, a calculation based on the conventional method was carried out, in which the criterion for the domination of Al_2O_3 growth is given by $|\Delta G_{Al/Fe\text{-}O/Nb}/5| > |\Delta G_{2Fe\text{-}Nb}/3|$. The result indicates that Al_2O_3 growth is favourable when more than 30 at % O is dissolved in niobium. The solid solubility limit of oxygen in niobium at 1500 K, however, is only about 3 at % and such a high density of oxygen does not dissolve in niobium. In other words, the conventional criterion indicates that Al_2O_3 growth using the residual oxygen in niodium is impossible.

For the Al/Ni–O/Nb system, numerical calculations on the reaction-rate criterion could not be carried out, because no thermodynamic data for the Ni–Nb reaction were available. However, the rate of Al_2O_3 growth is expected to be very slow, because the value of $|\Delta\mu/5|$ for Al_2O_3 growth in the Al/Ni–O/Nb system is only one-tenth of that in the Al/Fe–O/Nb system. Therefore, the domination of Al_2O_3 growth is expected to be difficult, unless the Ni–Nb solid solution is especially thermodynamically unstable.

5. Conclusion

The diffusion-preventive layer which is formed by heat treatment at the plasma-sprayed Nb/FeCrAlY interface is identified as Al_2O_3. A growth mechanism for the Al_2O_3 layer has been proposed, in which the origin of oxygen in Al_2O_3 is attributed to the residual oxygen in plasma-sprayed niobium. To justify the above model, numerical calculations based on thermodynamics were carried out. These showed that the 1–2 at % residual oxygen, which is usually involved in plasma-sprayed metals, in niobium is sufficient for Al_2O_3 layer growth. The calculations also show the reason why no Al_2O_3 growth is observed in the Al/Ni–O/Nb system.

Acknowledgements

The authors thank Mr Soma for his assistance in the computer operation, Mr Suzuki for the SEM/EPMA analysis, and Dr Iizuka for reviewing the original manuscript and encouragement of the research. They are also indebted to Mr Umibe for reviewing and giving comments to the original English manuscript.

References

1. D. W. PETRASEK, D. L. McDANIELS, L. J. WESTFALL and J. R. STEPHENS, *Metals Prog.* **130** (1986) 27.
2. M. W. KOPP, J. K. TIEN and D. W. PETRASEK, in "Superalloys 1988", edited by S. Reichmann, D. N. Duhl, G. Maurer, S. Antolovich and C. Lund (The Metallurgical Society, Warrendale, 1988) pp. 193–201.
3. R. WARREN, and G. S. UPADHYAYA, "Sintered Metal-Ceramic Composites" (Elsevier Science, Amsterdam, 1984).
4. M. ITOH, T. SUZUKI, M. NAKAHASHI and H. TAKEDA, in "Proceedings of the 102nd Meeting of the Japan Institute of Metals", edited by H. Shirai (The Japan Institute of Metals, Sendai, 1988) No. 492.
5. *Idem.*, in "Proceedings of the 103rd Meeting of the Japan Institute of Metals", edited by H. Shirai (The Japan Institute of Metals, Sendai, 1988) No. 692.
6. *Idem.*, in "Proceedings of the 105th Meeting of the Japan Institute of Metals", edited by H. Shirai (The Japan Institute of Metals, Sendai, 1989) No. 962.
7. R. H. PRAMOD, D. DONALD, T. HAWKINS, M. GLEISER and K. K. KELLEY, "Selected Values of the Thermodynamic Properties of Binary Alloys" (American Society for Metals, Metals Park, 1973).
8. "JANAF Thermochemical Tables" (National Bureau of Standards, 1965).
9. J. P. PEMSLER, *J. Electrochem. Soc.* **108** (1961) 744.

Received 5 November 1990
and accepted 25 February 1991